The potential of antifungal peptide Sesquin as natural food preservative

Francisco Ramos-Martín, Claudia Herrera-León, Viviane Antonietti, Pascal Sonnet, Catherine Sarazin, Nicola d'Amelio

The potential of antifungal peptide Sesquin as natural food preservative

Francisco Ramos-Martín[1,*], Claudia Herrera-León[1], Viviane Antonietti[2], Pascal Sonnet[2], Catherine Sarazin[1], and Nicola D'Amelio[1,*]

[1] Unité de Génie Enzymatique et Cellulaire UMR 7025 CNRS, Université de Picardie Jules Verne, Amiens, 80039, France

[2] Agents Infectieux, Résistance et Chimiothérapie, AGIR UR 4294, Université de Picardie Jules Verne, UFR de Pharmacie, Amiens, 80037, France

* To whom correspondence should be addressed. Tel: +33 3 22 82 7473; Fax: +33 3 22 82 75 95; Email: nicola.damelio@u-picardie.fr. Correspondence may also be addressed to francisco.ramos@u-picardie.fr.

Highlights

- Sesquin shows antimicrobial activity against fungi and bacteria involved in food spoilage.
- Based on NMR and MD data we have found that Sesquin interacts with biomimetic bacterial and fungal membranes.
- Sesquin specifically interacts with phosphatidylethanolamine and ergosterol altering membrane organization.
- A mechanism of action at atomic level is proposed explaining additional biological activities.
- MD data show that its activity is preserved at high pressure or with electric field pulses, commonly used as food preservation techniques .

ABSTRACT

Sesquin is a wide spectrum antimicrobial peptide displaying a remarkable activity on fungi. Contrarily to most antimicrobial peptides, it presents an overall negative charge. In the present study, we elucidate the molecular basis of its mode of action towards biomimetic membranes by NMR and MD experiments. While a specific recognition of phosphatidylethanolamine (PE) might explain its activity in a variety of different organisms (including bacteria), a further interaction with ergosterol accounts for its strong antifungal activity. NMR data reveal a charge gradient along its amide protons allowing the peptide to reach the membrane phosphate groups despite its negative charge. Subsequently, the peptide gets structured inside the bilayer, destabilizing its order. MD simulations predict that its activity is retained in conditions commonly used for food preservation: low temperatures, high pressure, or the presence of electric field pulses, making Sesquin a good candidate as food preservative.

Keywords: food biopreservation, antimicrobial peptide, antifungal, NMR, molecular dynamics, biomembranes

1. Introduction

Food preservation is hampered by the action of a variety of bacteria and fungi. Different preservation techniques have been developed, including fermentation, addition of salts or sugars, picking, drying, cooling, addition of preservatives, heating, modified packaging atmosphere, high pressure or even high electric fields [1–15]. Although these techniques have significantly improved the preservation of food, they have also stimulated the rise of resistant microorganisms able to survive under these extreme conditions. Among them, *Botrytis cinerea* and *Fusarium oxysporum* are among the most critical microorganisms because of their ability to affect common products such as wheat and grapes. *Botrytis cinerea* is a necrotrophic fungus, which causes widespread infection of grapes, tomatoes, strawberries, and other fruits [16]. It is also the most destructive pathogen on green and leafy vegetables. Its virulence, which involves pathogens and hosts inflammatory response [17], is amplified by its extreme tolerance to low temperatures[18]. Since *Botrytis* infects every plant part at any growth stage, the advantage of the use of fungicides is very limited[19]. *Fusarium oxysporum* is an opportunistic pathogen producing Fusarium wilt disease[20] and able to infect citrus fruit[21] but also vegetables such as potatoes, onions and garlic, among many others [16]. Most importantly, *Fusarium* sp. is the principal pathogenic fungal genus causing spoilage of maize, and producing mycotoxins harmful to humans and domestic animals [22,23].

In the attempt to develop new antifungals active against *Botrytis cinerea* and *Fusarium oxysporum*, we focused on Sesquin, an antifungal peptide homologous to Defensin that was isolated from *Vigna sesquipedalis* [24]. The use of antimicrobial peptides (AMPs) as antimicrobials is a promising strategy not only to treat health diseases but also to prevent the deleterious effects of pesticides in the environment [25]. In fact, they are already in use in the food industry because of their ability to control the growth of undesirable microorganisms while maintaining the qualities and nutritional properties of products [26]. Not only Sesquin attacks *Botrytis cinerea, Fusarium oxysporum* and *Mycosphaerella arachidicola* but also several bacteria (*Escherichia coli, Proteus vulgaris, Mycobacterium phlei* and *Bacillus megaterium*), cancer cells (MCF-7 breast cancer model and leukemia M1 cells) and viruses (human immunodeficiency virus-type 1 reverse transcriptase). Despite the exceptional variety of targeted organisms, the mode of action of Sesquin has not been deeply investigated [27]. A molecular picture of its interaction with fungal and bacterial membranes could explain why Sesquin displays wider spectrum activity than sequence-related peptides [28,29]. Studies on

membranes mimicking eukaryotic cells are also useful to predict possible undesirable cytotoxic effects for applications of Sesquin as a food preservative. As a food preservative, Sesquin does not appear to be cytotoxic. Unlike other PE-specific AMPs like cyclotides, maximin H and lantibiotics [30–32], Sesquin does not interact with phosphatidylcholine, making its mechanism of action unique and reducing its toxicity as compared with other PE-targeting peptides. In fact, contrarily to those peptides [33], Sesquin is not reported to be hemolytic probably due to the fact that PE is minimally exposed in healthy RBC (less than 1% [34]).

In this paper, we investigate a possible use of Sesquin as a food preservative by observing its effects on biomembranes of different compositions and in different conditions. By liquid and solid-state NMR and molecular dynamic simulations we describe the interaction of Sesquin with membranes mimicking fungi, bacteria and eukaryotic cells. A specific interaction with phosphatidylethanolamine might explain why, while unaffecting mammalian mimetic membranes, Sesquin displays such a wide spectrum activity. In particular, we show how a direct interaction with ergosterol could account for its strong antifungal activity. Finally, we investigate the compatibility of Sesquin with modern food preservation techniques such as high pressure, or the presence of electric field pulses.

2. Materials and Methods

2.1. Sequence alignment by ADAPTABLE web server

The families of peptides active against both *Botrytis cinerea* and *Fusarium* sp. were created by the family generator page of ADAPTABLE web server[35] using the following parameters: “Target Organism = fusarium, cinerea”; “Substitution matrix = Blosum45”; “Minimum % of similarity = 60; “Experimentally validated = yes”.

The family of peptides sequence-related to Sesquin (KTCENLADTY) was created by the family generator page of ADAPTABLE web server using “Create the family of a specific peptide” option with the following parameters: “Substitution matrix = Blosum45”; “Minimum % of similarity =70”.

As ADAPTABLE continuously updates with new entries, sequence-related families might change slightly with the time [35].

2.2. Synthesis of Sesquin

Fmoc(9-fluorophenylmethoxy)-amino acids and Fmoc-Tyr(tBu)-AC TentaGel® resin (0.22 mmol/g, particle size: 90 µm) were purchased from Iris Biotech (Germany). The other chemical compounds were purchased from VWR Chemicals, Iris Biotech or Acros and used without further purification. The peptides were synthesized on a CEM Liberty 1 Microwave Peptide Synthesizer, using standard automated continuous-flow microwave solid-phase peptide synthesis methods. Five-fold molar excess of the above amino acids was used in a typical coupling reaction. Fmoc-deprotection was accomplished by treatment with 20% (v/v) piperidine in N-methyl-2-pyrrolidone (NMP) at 75 °C. The coupling reaction was achieved by treatment with 2-(1H-benzotriazol-1-yl)-1,1,3,3-tetramethyluronium hexafluorophosphate (HBTU) and N,N-diisopropylethylamine (DIEA) in NMP using a standard microwave protocol (75 °C). The peptide was cleaved and side-chain deprotected by treatment of the peptide resin with a mixture of 1.85 ml of trifluoroacetic acid (TFA), 50 µL of triisopropylsilane, 50 µL H_2O and 50 mg of DL-dithiothreitol, in respective percent proportions, 92.5/2.5/2.5/2.5, during 4 hours at room temperature. The solid support was removed by filtration, the filtrate concentrated under reduced pressure, and the peptide precipitated from diethyl ether. The precipitate was washed several times with diethyl ether and dried under reduced pressure. The peptides were purified on an RP-HPLC C18 column (Phenomenex® C18, Jupiter 4µ Proteo, 90 Å, 250x21.20 mm) using a mixture of aqueous 0.1% (v/v) TFA (A) and 0.1% (v/v) TFA in acetonitrile (B) as the mobile phase (flow rate of 3 ml/min) and employing UV detection at 210 and 254 nm.

The peptide KTCENLADTY was obtained according to the precedent synthesis and purification procedures starting from the Fmoc-Tyr(tBu)-AC TentaGel® resin (454.5 mg, 0.100 mmol). Peptide was obtained, as a white powder, with a total yield of 45.3%, after purification by reverse-phase HPLC (97% analytical purity, Fig. S1).

2.2. Molecular Dynamics Simulations

Systems for simulations were prepared using CHARMM-GUI [36–38]. A total of 128 lipid molecules were placed in each lipid bilayer (i.e., 64 lipids in each leaflet) and peptide molecules were placed over the upper leaflet at a non-interacting distance (>10 Å). Lysine residues were protonated. Initial peptide structure was obtained from the SATPdb database

[39] (id: 24206). In the case of calculations with 8 peptides, they were placed next to each other but not in contact. A water layer of 50-Å thickness was added above and below the lipid bilayer which resulted in about 15000 water molecules (30000 in the case of CL) with small variations depending on the nature of the membrane. Systems were neutralized with Na^+ or Cl^- counterions.

MD simulations were performed using GROMACS software [40] and CHARMM36m force field [41,42] under semi-isotropic (for bilayers) and isotropic (for micelles) NPT conditions [43,44]. The TIP3P model [45] was used to describe water molecules. Each system was energy-minimized with a steepest-descent algorithm for 5000 steps. Systems were equilibrated with the Berendsen barostat [46] and Parrinello-Rahman barostat [47,48] was used to maintain pressure (1 bar) semi-isotropically with a time constant of 5 ps and a compressibility of 4.5×10^{-5} bar^{-1}. Nose-Hoover thermostat [49,50] was chosen to maintain the systems at 310 K or 278 K with a time constant of 1 ps. High pressure simulations were performed at 1000 bar pressure level as reported in other works [51]. Simulations under electric fields were run setting a static field with E_0= 0.1 V/nm in the Z-direction [52]. All bonds were constrained using the LINear Constraint Solver (LINCS) algorithm, which allowed an integration step of 2 fs. PBC (Periodic Boundary Conditions) was employed for all simulations, and the particle mesh Ewald (PME) method [53] was used for long-range electrostatic interactions. After the standard CHARMM-GUI minimization and equilibration steps [43], the production run was performed for 500 ns and the whole process (minimization, equilibration and production run) was repeated once in the absence of peptide and twice in its presence. Convergence was assessed using RMSD and polar contacts analysis.

All MD trajectories were analyzed using GROMACS tools [54,55] and Fatslim [56]. MOLMOL [57] and VMD [58] were used for visualization. Graphs and images were produced with GNUplot [59] and PyMol [60].

2.3. Sample preparation, NMR experiments and analysis

Backbone and sequential resonance assignments were achieved by ^1H,^{13}C-HSQC, ^1H,^1H-TOCSY (mixing of 60 ms), and ^1H,^1H-NOESY (mixing of 200 ms) recorded on a 500 MHz Bruker spectrometer equipped with a 5 mm BBI probe. Deuterated sodium 3-(trimethylsilyl)propionate-d4 (TSP-d4) at a concentration of 100 µM was used as internal

reference for chemical shift. Reference random coil values in our experimental conditions (T = 278 K, pH 6.6 and ionic strength 0.01 M) were calculated by POTENCI web server (https://st-protein02.chem.au.dk/potenci/) [61].

A 0.8 mM sample of Sesquin (90% 10 mM phosphate buffer / 10% D_2O, pH 6.6) was titrated with a 1 M stock solution of DPC:d38 to a final DPC concentration of 60 mM. Titration was followed by 1D ^{1}H-NMR at 278 K. For the assignment of the interacting form of the peptide 2D ^{1}H,^{1}H-NOESY and ^{1}H,^{13}C-HSQC were recorded at total DPC concentrations of 60 mM.

Bicelles were prepared as follows. A mixture of 33.3 % DMPC and 66.7 % DHPC in chloroform was used to obtain isotropic bicelles at a molar (q) ratio of 0.5. The solvent was evaporated under a nitrogen flow and the samples were then lyophilized and resuspended in a 10 mM phosphate buffer (pH 6.6) to reach a final concentration of 1 M (stock solution). DMPG, DMPS and DMPE containing bicelles were prepared as described above, except part of DMPC was replaced by DMPG (25%), DMPS (25%), DMPE (10%) or ergosterol (5%) reproducing previous experiments [62–65]. A 0.8 mM sample of Sesquin (90% 10 mM phosphate buffer / 10% D_2O, pH 6.6) was titrated with bicelles up to a final lipid concentration of 70 mM and monitored at 278 K by a 1D ^{1}H-NMR spectrum recorded after each addition.

Multilamellar vesicles (MLVs) containing deuterated palmitoyl chains were prepared according to the conventional protocol [66–70] using the following proportions: 50%:50% POPC/POPC:d31, 50%:50% POPG/POPG:d31, 50%:50% POPS/POPS:d31; 70%:30% POPE:d31/POPG , 50%:50% CL/POPC:d31 , 70%:30% POPE:d31/POPC, 70%:25%:5% POPE:d31/POPC/Ergosterol, 67%:27%:6% POPE:d31/POPG/CL, 50%:50% POPC:d31/SoyPI. Lipids were solubilized in chloroform and solutions were mixed in order to obtain the right proportions in a total lipid amount of 60 mM. The resulting solution was evaporated under nitrogen gas flow. The sample was hydrated with ultrapure water, well-vortexed to promote total hydration and lyophilized overnight to remove the traces of solvents. The resulting powder containing lipids was hydrated by 80 µl of ultra pure water (for non charged lipids) or 10 mM phosphate buffer pH 6.6 100 mM NaCl (for charged lipids), vortexed and homogenized using four free-thaw cycles involving one step of freezing (-80°C, 15 min) followed by thawing (40°C, 15 min) and shaking. Finally, the MLV samples were placed in a 7-mm ssNMR rotor to perform the experiments. 2.4 mM of peptide were added for interaction studies.

ssNMR experiments were recorded at 310 K, 298 K and 283 K on a Bruker Avance Biospin 300 WB (7.05T) equipped with a CP-MAS 7-mm probe. Static ^{2}H NMR was carried out applying a phase cycled quadrupolar echo pulse sequence (90°x-τ-90°y-τ-acq) [71]. The parameters used are: spectral width of 150 kHz, π/2 pulse of 5.25 µs, an interpulse delay of 40 µs, a recycled delay of 1.5 s, and a number of acquisitions ranging from 8 k to 14 k depending on samples. For all spectra, an exponential line broadening of 100 Hz was applied before Fourier-transform from the top of the echo signal.

3. RESULTS AND DISCUSSION

3.1. Property alignment highlights motifs potentially involved in Sesquin wide-spectrum activity

There exist more than 6000 antifungal peptides, out of which about 200 display significant activity towards both *Botrytis cinerea* and *Fusarium* sp. (e.g. IC_{50}<10uM). Sequence alignment by ADAPTABLE web server[35] grouped peptides active against these fungi in sequence-related families (SR families). Out of these, we selected the family generated by Sesquin shown in Figure 1A, for its simplicity (only 10 amino acid long) and its interesting properties. Sesquin is in fact not only antifungal but also antibacterial, anticancer and antiviral. The alignment reveals that a few motifs are particularly conserved: the initial K, the CEN triad and the D residue (Figure 1B). Using Sesquin as a bait to find similar sequences, independently of the activity resulted in the creation of the SR family with members which might also be active against *Botrytis cinerea* and *Fusarium* sp., even though they might not have been tested yet (Figure 1C). This latter alignment reveals that Sesquin is similar to a significant number of antimicrobial or anticancer peptides, in part belonging to the Defensin family, where it is often found at the N-terminus of much longer sequences. Their activities are mostly antifungal, antiviral and antibacterial but also anticancer and antiparasitic. It should be noted that Sesquin is an atypical antimicrobial peptide as it has a negative overall charge and is too short to form stable alpha-helices, although a hypothetical helix would have amphipathic character (Figure 1D).

3.2. Sesquin is substantially unstructured in solution NMR

In order to get insight into the mechanism of action of Sesquin, we analyzed the structure of the peptide in solution by NMR spectroscopy. Antifungal peptides commonly adopt a random coil or alpha helical conformation, while they rarely assume extended strand and beta-turn conformations[72]. 2D-NOESY, 2D-TOCSY and ^{1}H-^{13}C HSQC experiments were acquired for complete ^{1}H, ^{13}C resonance assignment of backbone amide protons and non-exchangeable CH moieties (Table S1). The analysis of the NOESY spectrum did not reveal the presence of NOE effect between protons distant in the primary structure, suggesting that the peptide is completely unstructured in solution. Accordingly, the ^{1}H amide region of the NMR spectrum improves in quality at low temperature, as expected by a slowing down of exchange phenomena with the solvent. A further confirmation comes from the Chemical Shift Index (CSI)[73–75] (Figure 1E) showing very limited deviations from random coil values of Hα, Cα and Cβ atoms, which are lower than the threshold (0.1 ppm for ^{1}H and 0.7 ppm for ^{13}C)[76].

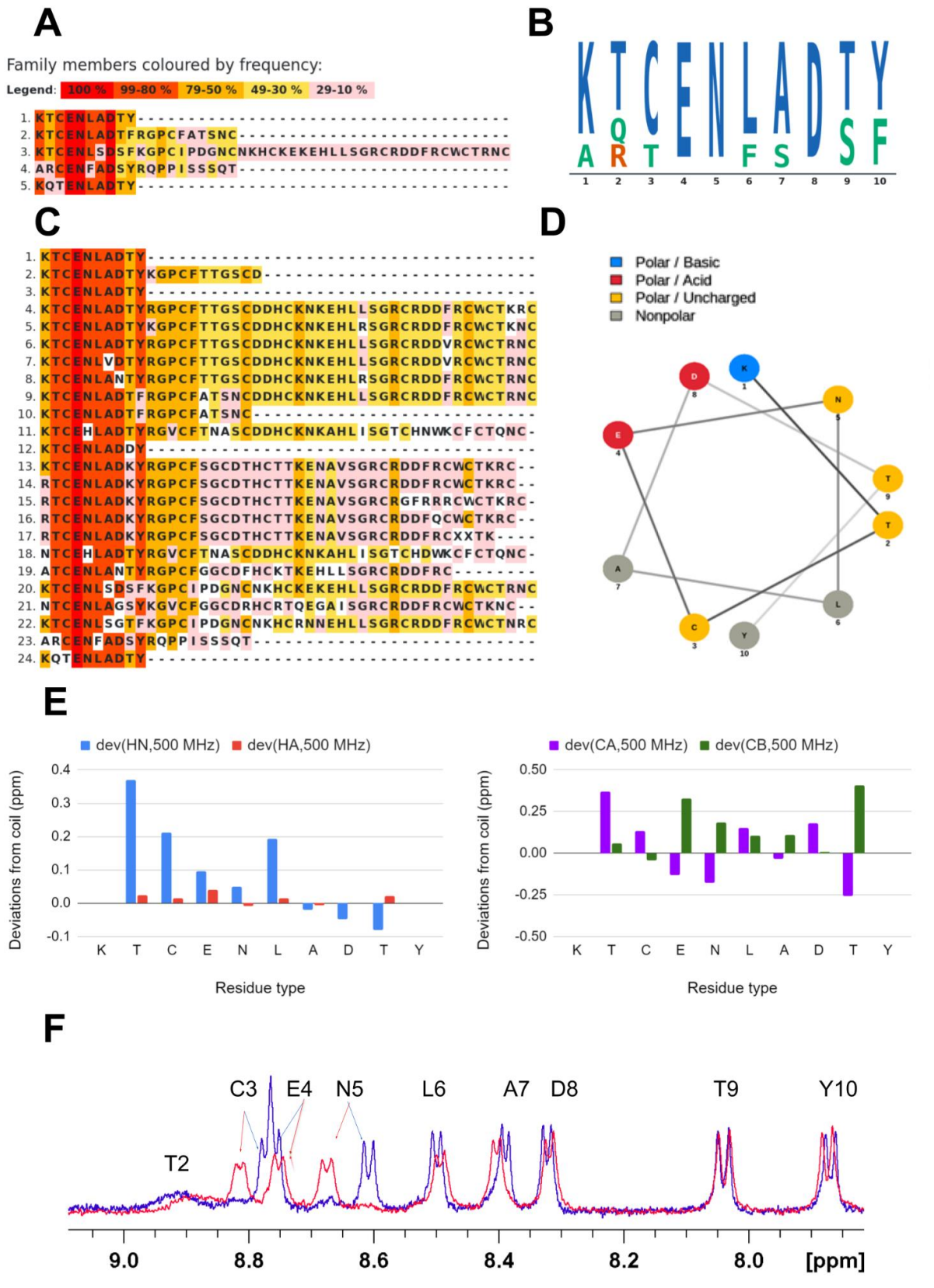

Figure 1. *(A) Sequence-related family generated by ADAPTABLE using Sesquin as a bait among peptides with IC_{50}<10µM against both Botrytis cinerea and Fusarium sp. (B) Relative importance of each aminoacid in terms of conservation. (C) Sequence-related family*

generated by Sesquin used as a bait among the full ADAPTABLE database, independently of their activity. (D) Helical wheel plot (generated by NetWheels [77]). (E) Chemical shift deviations from random coil values of HN, Hα, Cα and Cβ atoms. (F) Amide region of ^{1}H NMR spectrum for the reduced (blue) and oxidized (red) forms of Sesquin.

We also investigated the influence of the cysteine residue on the structure of the peptide and the possible formation of disulphide-linked dimers. The NMR spectrum of Sesquin does change after a few days in solution and changes are reverted by the addition of reducing agents such as dithiothreitol (DTT) or tris(2-carboxyethyl)phosphine (TCEP). The chemical shift of beta carbon of cysteine changes from 41.2 ppm to 28.2 ppm, definitively confirming the formation of disulfide bonds [78]. As shown in Figure 1F, oxidation perturbs the chemical shift of the amide region in a very specific region of the molecule that involves the cysteine and its neighbouring aminoacids. No other important changes are observed, indicating that the dimer remains substantially unstructured.

3.3. The chemical shift of amide protons reveals a peculiar electronic distribution in Sesquin

The values of chemical shifts indicate that amide protons in Sesquin appear progressively shielded from residue T2 to Y10 (K1 is not detected). With the exception of L6, also the deviations from random coil values (Figure 1E) confirm this peculiar trend. This indicates that the electronic density at the level of amide protons increases from the first to the last residue, possibly leaving on the former a substantial positive charge. Such a peculiar charge distribution might have a role in the interaction with its target (see section 3.7).

3.4. Interaction with model membranes

3.4.1. Studies with DPC micelles suggests poor affinity for PC head groups

The interaction of Sesquin with dodecylphosphocholine (DPC) micelles was followed by NMR, to ascertain its tendency to assume secondary structure in their hydrophobic cores. Micelles allow the study in solution and provide a very rough model of the apolar environment within biological membranes. Contrary to other peptides [79,80] and despite the complementary charges of the exposed choline groups, Sesquin does not seem to interact

with DPC micelles (Figure S2), suggesting its poor affinity for the hydrophobic environment found in bilayers and the absence of a specific recognition of PC headgroups. Isotropic bicelles and liposomes are more realistic models, allowing to evaluate the interactions with a wider variety of phospholipids, able to better reproduce the membranes of different organisms [62,81].

3.4.2. Studies with isotropic bicelles suggests an interaction with PE head groups

With respect to micelles, isotropic bicelles allow a certain degree of control on its lipid composition, providing a better model for biological membranes still amenable to studies by solution state NMR [62,81]. Also in this case, Sesquin showed a relative insensitivity to the presence of bicelles of various compositions (Figure S3A). Weakening of peaks in the HSQC spectra (Figure S3B) is partly attributable to partial oxidation of the sample during the experiments or artifacts due to the presence of bicelles, whose lipids are much more concentrated than the peptide (we used a peptide: lipid ratio of 1:25 and the result did not change even with a ratio of 1:80). On the other hand, peaks relative to the N terminus (Hα/Cα of residues T2, C3, E4) tend to disappear and the effect is more evident in the presence of DMPE, suggesting a preference for phosphatidylethanolamine (Figure S3B, bottom). The presence of a conserved Cys residue could indicate a possible role of disulphide bonds in the mechanism of action. However, the oxidised form of Sesquin remains quite insensitive to the presence of bicelles, possibly displaying a weak interaction with DMPC/DHPC bicelles (Figure S3B, top).

3.4.3. Studies with MLVs show Sesquin preference for fungal and bacterial lipids

Multilamellar vesicles (MLVs) or liposomes provide more realistic models of biological membranes in that they allow phospholipid mixtures incompatible with bicelles or micelles. Thanks to their properties, we have been able to study their interaction with Sesquin at variable temperatures (in a range from 283 K to 310 K) and using a wide range of lipid compositions mimicking membranes of different organisms.

Static ^{2}H NMR of liposomes provides valuable information on the internal dynamics of the bilayer when the acyl chains of phospholipids are deuterated. For a matter of simplicity in spectra interpretation, we performed our measurements on phospholipids deuterated only

in the palmitoyl chain. Each ^{2}H atom presents a quadrupolar splitting whose magnitude scales with its dynamics, due to averaging of orientations with respect to the external magnetic field [82–84]. As a consequence, ^{2}H atoms in very mobile molecular fragments, as methyl groups, display small quadrupolar splitting and appear at the center of the spectrum. Conversely, ^{2}H atoms located in the rigid part of the acyl chain, as well as those found close to the ester bond (the plateau region including carbon atoms 2-6), display almost full couplings and appear at the edges of the spectrum. Insertion of molecules in the bilayer is usually accompanied by a change in the degrees of freedom of acyl chains and can be used as an indirect experiment to probe the depth of the interaction [85,86]. The peptide may have a rigidifying or fluidifying effect, monitored as an increase or a decrease in the width of the ^{2}H spectrum, respectively [84,87–91].

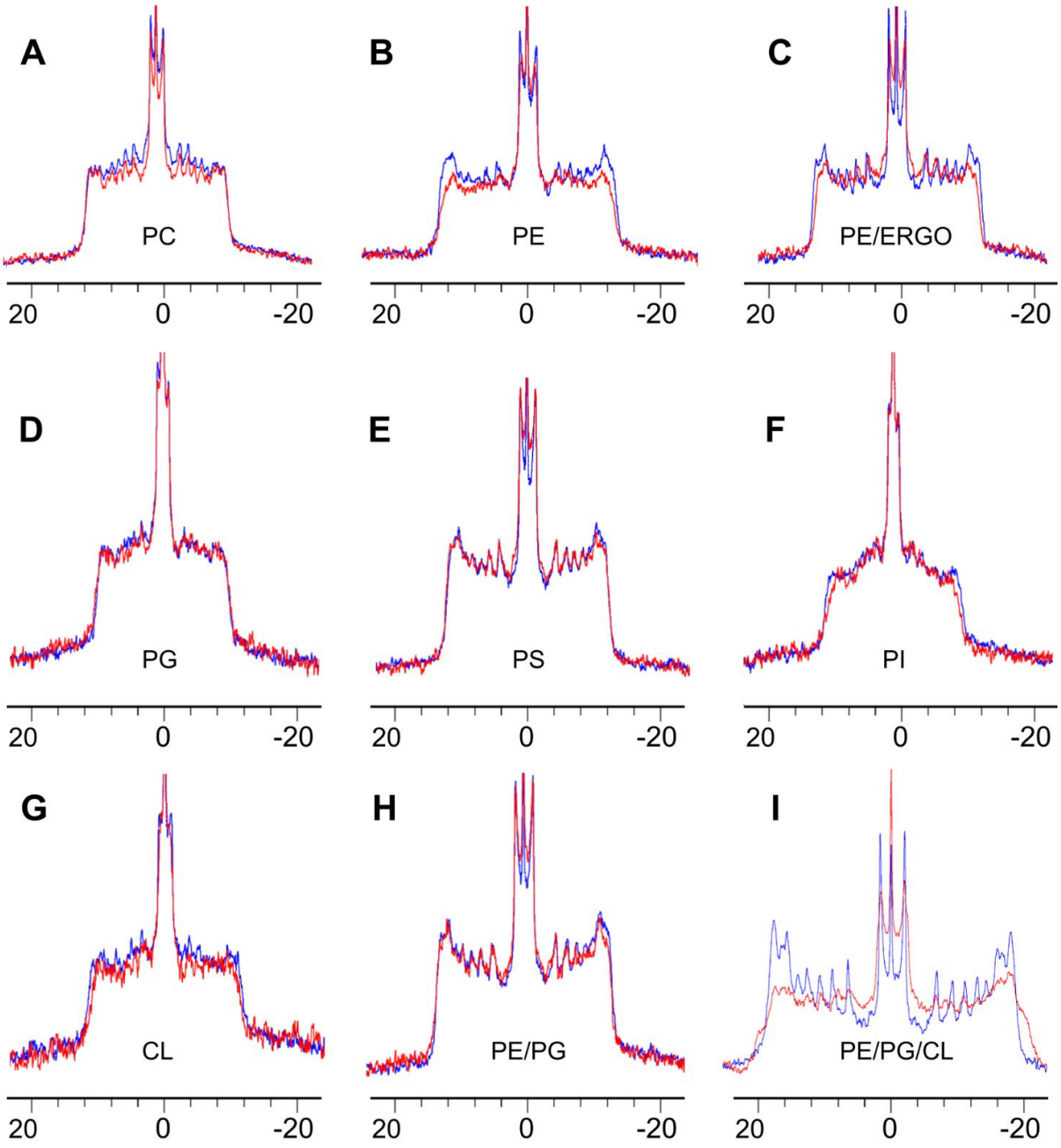

Figure 2. *Static ^{2}H NMR spectra of various MLV liposomes in the absence (blue) and the presence (red) of Sesquin.*

Among the large variety of liposome types tested (Figure 2), a clear fluidifying effect is observed with PE (Figure 2B) over PC (Figure 2A). Note that PE solutions must contain at least a small percentage of PC (see Material and methods section) for the correct assembly of liposomes [92–99]. The effect is conserved in the presence of ergosterol, which was added to PE liposomes to better model fungal membranes [100–104]. The presence of ergosterol slightly reduces the fluidification induced by Sesquin (Figure 2C), proportionally to its

concentration (Figure S4). Analyzing liposomes with different phospholipid compositions, we observed small effects for PI (Figure 2F) and CL (figure 2G), typically found in fungal [103,105,106] and bacterial membranes (but also mitochondrial)[107–110], respectively, while not for pure PG and PS (Figures 2D,E). This is an interesting observation as Sesquin targets several bacteria, although with lower activities than fungi [24].

Bacterial membranes are typically composed of a mixture of PE, PG and CL [107–110]. Our experiments with mixed lipid compositions show that Sesquin has an important fluidification effect on such type of liposomes (Figure 2I) but is not able to perturb the internal dynamics of PE/PG bilayers (Figure 2H), probably because of the richer network of interactions that the peptide would need to break for its insertion[108,111]. The addition of CL in PE/PG bilayer rigidifies the membrane significantly as demonstrated by the increase in the overall width of the spectrum (compare Figure 2H and figure 2I) while breaking some of these interactions [112]. As a consequence, the peptide might penetrate more easily causing a change in fluidity even more apparent.

3.5. Molecular dynamics studies on phospholipid bilayers confirm a specific recognition of PE

Molecular dynamics (MD) simulations were performed to study Sesquin interaction with various bilayers. While other techniques and sampling algorithms are better suited for the detection of processes needing a longer time scale to occur [113–119], MD still allows us to better understand the mechanism of action of this peptide at the first stages of the interaction and to study a wider range of membrane lipid compositions otherwise harder to achieve experimentally. MD also permits a direct comparison with NMR data, providing a molecular picture for their interpretation.

Snapshots of characteristic peptide-membrane interactions are shown in Figure 3. In our simulations, Sesquin does not show an affinity for POPC membranes (Figure 3), although the two-fold positive N-terminus might be electrostatically attracted to the negatively charged phosphate groups of POPC. Likewise, another electrostatic interaction could potentially be established between the choline group and the side chains of E4 and D8, which are deprotonated at physiological pH. The absence of interaction is probably due to the steric hindrance of the choline headgroup, which does not allow distances sufficiently short for a

significant Coulombic attraction. This result is consistent with the absence of relevant interaction with the PC headgroup observed by liquid and solid-state NMR (Figures S2, S3 and 2).

In POPE membranes (Figure 3), this steric hindrance is removed (the three methyls of choline are replaced by three hydrogen atoms) and the interactions hypothesized above are allowed to take place: we observe the formation of a salt bridge between the amine groups of K1 with the negatively charged oxygen atoms of the membrane phosphates and between the carboxylates of E4, D8 and of the C-terminus with the positively charged amine group of POPE. In order to have a more quantitative analysis of such interactions, we calculated the radial distribution function[45] of each N, O atom of the membrane with respect to each N, O atom of the peptide and we extracted the maximum of these curves within the H-bond/salt-bridge distances. The obtained values for each couple of polar atoms (Figures S5-S7) give an estimate of the frequency of such interactions along MD trajectories and, consequently, of their probabilities. Results in Figure S5 show very clearly that Sesquin approaches the membranes with its N-terminus but, with the exception of POPE, it is not able to establish a stable interaction involving its complete sequence. The frequency of the interaction is very poor in POPC (even the most frequent, between the N-terminus of Sesquin and one oxygen of its phosphate, occurs rarely) while it becomes important in POPE. In this case, the most frequent interaction is between the lysine side chain of Sesquin and one oxygen of its phosphate. Most importantly, Figures 3 and S5-S9 show that Sesquin interacts entirely with membranes (and not only with its N-terminus) uniquely when POPE is present because only POPE (and POPS) provide an accessible positively charged group that can interact with its negatively charged groups (E4, D8 and the C-terminus). In the case of POPS (Figure S5), the carboxylate of serine headgroup probably reduces the accessibility of Sesquin and/or weakens the electrostatic interaction with the amine of POPS. Accordingly, most of the interactions established by negatively charged carboxylates of Sesquin with POPE are lost with PS.

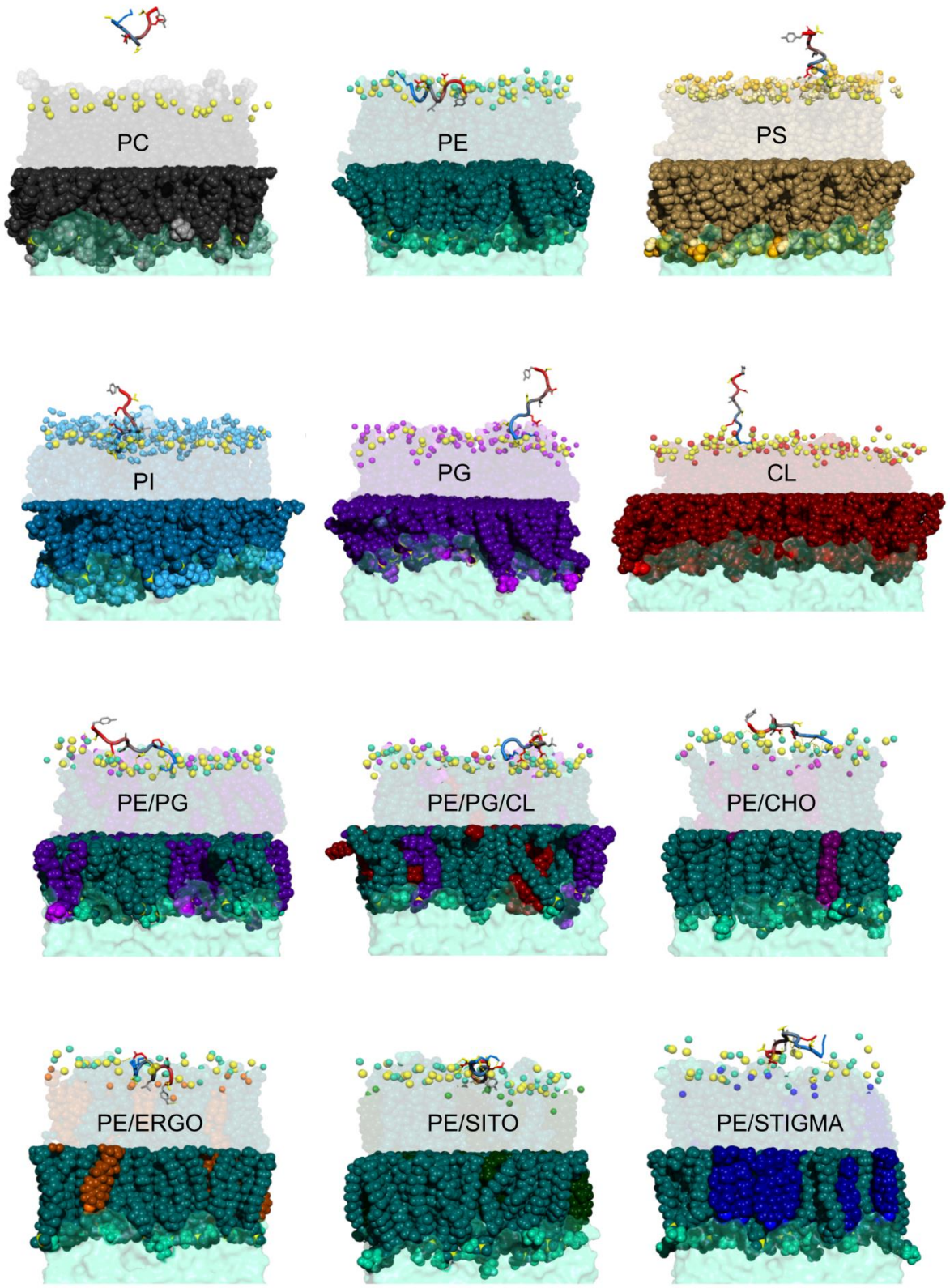

Figure 3. *MD snapshots showing Sesquin at characteristic distance from several membranes with variable phospholipid compositions. Color code: phosphorus atom: yellow. POPC black (body) and light gray (choline group); POPE dark green (body), turquoise (headgroup), light green (amine of the headgroup); POPS brown (body), gold (headgroup), light yellow (amine of*

the headgroup) and orange (carboxyl of the headgroup); POPI blue (body), light blue (headgroup), cyan (hydroxyls of the headgroup); POPG dark violet (body), violet (headgroup), light violet (hydroxyls of the headgroup); CL dark red (body) and light red (headgroup); CHO purple (body) and light purple (hydroxyl); ERGO dark orange (body) and light orange (hydroxyl); SITO deep-dark green (body) and pea-green (hydroxyl); STIGMA electric blue (body) and light electric blue (hydroxyl). For clarity, only functional groups of headgroups are represented as spheres in the upper leaflet. Sesquin is shown as "tube" representation, colored from blue (N-terminus) to red (C-terminus). Side chains are shown as sticks with the following color code: positively charged (blue), negatively charged (red), non-polar (light gray), polar (yellow).

A remarkable affinity for PE containing membranes is confirmed by a deep insertion of the peptide, highlighted by a significant amount of apolar contacts (Figure S8). This phenomenon is observed not only in pure PE membranes but also with bacterial biomimetic membranes containing PE and in most PE based membranes with different sterols (Figures S9 and S10).

In the case of POPI, the network of interactions shown in Figure S6 is very simple as compared to other cases. Despite the steric hindrance of the inositol ring, the interaction between the N-terminus of Sesquin and one oxygen of POPI phosphate is frequent (Figure S6). No other significant interactions are observed while NMR data suggest a slight fluidification of POPI containing MLVs (Figure 2F).

In the case of POPG, the oxydrils in the headgroup do not seem to be involved in specific H-bonds and Sesquin interacts sporadically with only its N-terminus (Figure S5), without being able to penetrate the bilayer (Figure S8), as experimentally confirmed (Figure 2). The situation is different with CL, despite the similarity of the functional groups in the two lipids. In this case, the oxygen atoms of the phosphate groups (OP13, OP14, OP33 and OP34) are accessible and readily available for interaction and Sesquin can bind them in bidentate fashion by using both its N-terminal and K1 side chain amines (Figure S6). Even if the interaction remains superficial (Figure S9), the geometry of CL makes Sesquin closer to the acyl chains of the bilayer.

3.6. The antifungal activity of Sesquin seems to involve a specific recognition of both PE and ergosterol

If our data have revealed an enhanced preference of Sesquin for PE phospholipid, it should be noted that PE is present in many different organisms and this specificity can explain Sesquin activity towards a wide range of organisms (not only fungi but also bacteria, virus [33,120–123] and cancer cells [33,124–127]). We therefore decided to investigate the effect of other lipids in POPE bilayers (Figure 3) and reproduce the composition of fungal (POPE/ERGO) [100] and bacterial (POPE/POPG or POPE/POPG/CL) membranes. The effect of sterols found in plants (SITO or STIGMA)[128] or vertebrates (CHO) was also studied to evaluate potential additional specificities.

In all cases, Sesquin interacts extensively, making a wide network of interactions with the membranes (Figure S6 and S7). The detailed behavior of Sesquin varies significantly from case to case. In bilayers representing bacterial membranes, a preference for PE over PG can be observed (Figure S6). When CL is present, the affinity increases significantly but interactions with CL predominate over PE.

An interesting aspect emerging from simulations is the formation of alpha helical structures in some POPE containing membranes. In most simulations, Sesquin is unstructured and quickly loses the initial alpha helical conformation predicted by the SATPdb database [39]. However, such helical structure reforms in POPE, ergosterol-containing POPE (typical of fungi) and sitosterol membranes (Figure S11 and S12). In other words, the amphipathic character of Sesquin created by the helical conformation (Figure 1D) is probably necessary for its action and could explain why Sesquin is a more potent antifungal than antibacterial. Figure 3 clearly shows that when a helix is formed, Sesquin can penetrate much deeper and establish polar contacts from the interior (the positive side chain of K1 with the phosphate oxygen atoms and the negative side chains of E4 and D8 with the amine groups of PE), thus destabilizing the membrane order. If the helix is not formed, the peptide still interacts but remains outside the bilayer. Once in the membrane it may act as other common AMPs [129]. As its short length does not allow encompassing the full membrane for the formation of a channel, Sesquin may be viewed as a PE specific AMP acting on membrane by carpet model [27].

Even if outside the scope of this work, it is interesting to point out that the selectivity for PE is able to explain its anticancer activity, due to the fact that apoptotic cancer cells and mitochondria of carcinogenic cells[130] tend to expose PE on their outer leaflet [33,124–127]. In a similar way, Sesquin could disrupt the envelope of HIV explaining its antiviral activity [33,120–123], although this has been ascribed to a direct interaction with the HIV reverse transcriptase.

Focusing on its antifungal properties, we need to take into account the activity in the presence of ergosterol, the most common fungal sterol [100]. Despite their relatively similar structure, we found an apparent preference of Sesquin for ergosterol. Such an affinity is highlighted by the presence of both polar and apolar contacts (Figures S7 and S10), but also a perturbation of the area per lipid (Figure S13 and S14) and the order parameter of the POPE palmitoyl side chains S(CD). The latter expresses the order of CH moieties in phospholipid acyl chains. It can be measured as a reduction of the quadrupolar splitting in NMR ^{2}H spectra [82,84,131] or calculated in MD simulations (Figure S15).

In particular, Sesquin can form polar contacts between the T2 or C3 side chains and the hydroxyl of ergosterol (Figure S7) that were not found with other sterols. As mentioned above, Sesquin folds into a helix only in the presence of sitosterol and ergosterol (Figure S12), but penetrates more deeply in the latter case (Figure S10) for which direct peptide-sterol contacts are observed, thus explaining the different effects on the order parameter (Figure S15). In the case of cholesterol and stigmasterol, Sesquin never penetrates deeply, probably due to the increased rigidity conferred by these sterols [84,132] (higher values of the order parameter in Figure S15). The preference for ergosterol over other sterols might be due to the slightly different geometry of its condensed ring body, caused by the introduction of a double bond between carbons 7 and 8 making the overall shape more planar than the other sterols (see the comparison with cholesterol in Figure S16).

3.7. A linear gradient of charge to approach the membrane and an amphipathic helix for its disruption

As discussed in section 3.3, NMR data indicate a progressive decrease in electronic density towards Sesquin N-terminus. In simulations, we observe that the peptide approaches the membrane as an arrow (see Figure 4) inserting in the membrane either the side chain or the

terminal amine of K1. Subsequently, the peptide folds into alpha helical conformation which allows the establishment of salt bridges with the amine of PE headgroups. By clinging to such a group with the carboxylates of E4 and D8 (which reside on the same side of the helix), hydrophobic side chains on the opposite side “fall” into the hydrophobic core. Subsequently, other interactions can be formed including a further salt bridge between the amine of PE and the carboxy terminus.

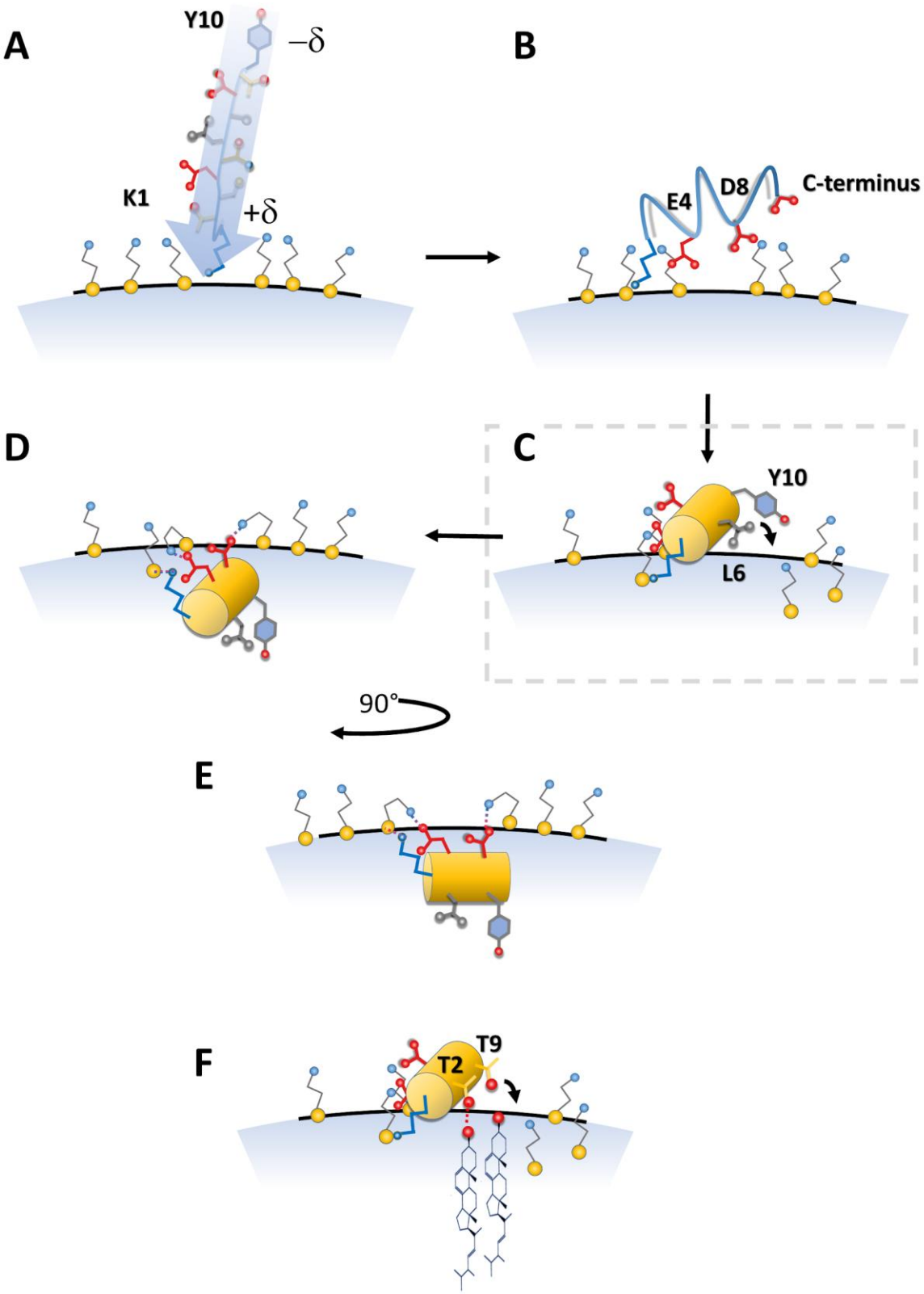

Figure 4. *Schematic representation of the mode of action of Sesquin peptide approaching targeted membranes. (A) Sesquin approaches the target membrane by forming a salt bridge*

between the N-terminal and/or its side chain amine and the negatively charged phosphate moieties of phospholipids (yellow spheres). A gradient of electron density (shown as an "arrow") amplifies the positive charge at the N terminus. (B) The interaction is stabilized by salt bridges between the carboxylates of E4 and D8 (red spheres), forming salt bridges with the amine moiety of PE head groups (blue spheres). (C) These interactions also stabilize the formation of an alpha helical conformation bringing E8 and D4 on the same side of an amphipathic helix, exposing hydrophobic residues L6 and Y10 towards the interior of the lipid bilayer. (D) As a consequence, the helix flips inside the bilayer, maintaining the salt bridges previously formed. (E) The same complex shown in D with a view rotated by 90 degrees. (F) In the presence of ergosterol a further interaction takes place in step C (framed with a dashed line), between oxydrils of the side chain of T2 (but also C3) and that of the sterol (red spheres). T9 is on the same side of the helix as T2 but does not seem to participate in the recognition.

A possible cooperative effect was explored by performing the simulations with 8 peptides per system. Although Sesquin tends to form aggregates by approaching the hydrophobic surface in helical conformation, each peptide seems to act independently in the first stages of the interaction with the membrane. The overall effect on the membrane can be better evaluated by calculating the area per lipid (Figures S13 and S14). In the case of PE-containing membranes the ensemble of the peptides exert a significant pressure on the surface, invaginating the bilayers as demonstrated by the increase and decrease of the area per lipid of the outer and inner leaflet, respectively.

3.8. A potential food preservative

For its unique properties as antifungal and antibacterial and the lack of hemolytic or cytotoxic activities [24], we have investigated the effect of some of the most used food preservation techniques on the molecular properties of Sesquin. In particular we have focused on temperature and pressure changes but also on the usage of electrical pulses. MD simulations have shown to be suitable to study novel food processing technologies such as high pressure and electric fields in combination with antimicrobial peptides [51,133–137].

When lowering the temperature to 278 K, some membranes undergo phase transitions, namely POPE (T_m=298 K) and POPS (T_m=287 K). Others approach the phase transition: POPC (T_m=271 K) and POPG (T_m=271 K) [138]. With the exception of CL (T_m=345 K), all other systems are significantly more rigid [139]. In this conditions, two effects play a role in the mode of interaction: (i) due to the decreased kinetic energy available at lower temperature, Sesquin tends to reside longer on membrane surfaces, establishing similar polar contacts as those described at 310K (Figures S17-S19); (ii) due to the increased rigidification of the membrane, Sesquin tends to penetrate less in the bilayers (Figures S19-S21). The first effect determines invagination of the membrane with one or multiple peptides (see the effect on the area per lipid, Figures S22 and S23) while the second effect significantly reduces the amount of apolar contacts with the acyl chains of phospholipids (Figures S19-S21). Overall, Sesquin penetrates only in pure PE, PE/ergosterol and in pure CL membranes where the acyl chains are directly accessible for the absence of a large headgroup.

While our simulations at 310 K did not reveal a specificity for POPI, at 278 K a clear reduction of the order parameter is observed only for this type of membranes (see Figure S24), demonstrating that Sesquin does not need to insert deeply in the POPI bilayer to fluidify it.

Pressure has been used as a way to preserve food [6,140]. Some of the advantages of this approach are the short process times[141], energy saving, and a good conservation of organoleptic properties [142]. High pressure has also been tested to prevent prions contamination [143,144]. On the other hand, some organisms including fungi [142,145] are tolerant to high pressures [146–148], or express resistance genes to tolerate such conditions [149,150]. Combination with other agents, as AMPs, could help to overcome these issues.

Under high pressure conditions and in the absence of Sesquin, we observe a significant decrease of area per lipid (data not shown) and an increase in the order parameter of acyl chains (Figure S25), in some cases due to the induction of phase transitions. Electron density profiles comparing the different membranes under atmospheric and high pressures (1000 bar) were also evaluated (see Figure S26). For most of the membranes (except for those undergoing phase transitions like POPE and POPS) it can be seen that densities are slightly lower at the two peaks corresponding to the lipid head groups while higher at the central

region. This would indicate a reduction in the volume in the center of the bilayer, while it is harder to compress further the more dense regions close to the head groups. Such effects were previously described in the literature for POPC and DOPC [51]. Pure POPE and POPS membranes undergo a phase transition at these high pressure conditions, leading to more remarkable changes in the profiles (Figure S26).

When a high pressure is applied in the presence of Sesquin, behaviors similar to those described at low temperature are observed but in this case the rigidification of the membrane can be dramatic, independently of the phase transition temperature. As a consequence, larger perturbations of the area per lipid are observed for PE, PE/ergosterol, PI and PS (compare Figures S27 and S28 with Figure S29) while the peptide penetrates poorly in all bilayers (Figures S30-S32) with the notable exception of PE and PE/ergosterol bilayers. This confirms the selective preference of Sesquin for fungal-like membranes and its possible use under high pressure conditions, allowing a synergistic effect aiming at destroying recalcitrant bacterial or fungal cells.

An emerging technique for food preservation is electric field processing. It has been successfully used with liquid or semi solid food such as milk, youghourts, soups and liquid eggs. In the last years it has been extended to solid meals [151]. Additionally, this technique has shown its capacity to preserve nutritional properties such as the vitamins content [10,13,15,152–156]. At variance with the previously described preservation methods, electric fields fluidify membranes (Figure S33) rather than making them more stiff, thus favouring the penetration of Sesquin. The choice of the electric field strength was dictated by the need to weaken the studied bilayer without disrupting it by its sole action. The analysis of polar and apolar contacts clearly show that electric fields amplify the antimicrobial effect of Sesquin (Figures S34-S38). In these conditions, Sesquin clearly lowers the order parameters of palmitoyl acyl chains (Figure S39) in PE and PE/Ergosterol bilayers due to its penetration in their inner cores. In parallel, the antibacterial properties are amplified with the establishment of polar and apolar contacts with all phospholipids present in bacterial membranes (PE,PG and CL) and their mixtures. It is worth pointing out that POPC bilayers (here representing mammalian membranes) remain poorly perturbed by the presence of the peptide even in such conditions. The use of Sesquin could allow lowering the power of electric fields

commonly used for food preservation with benefits for food integrity, organoleptic properties and lower energy consumption.

4. Conclusions

While we chemically synthesized Sesquin for our mechanistic study, applications should take into account strategies to make the production costs feasible such as its synthesis via fermentation. Once the ecological impact on fields is ascertained, applications in crop-protection could also be postulated by bioengineering of symbiotic bacteria although this is beyond the scope of the present workUnlike most antimicrobial peptides, Sesquin is a negatively charged molecule. Such a feature is the key for its specificity towards phosphatidylethanolamine headgroup, which contains a positively charged amine group. The overall negative charge of Sesquin is limited to -1 at physiological pH which could be a compromise between attraction to the PE amine groups and the overall negative charge, typically found in fungal membranes. In Sesquin, the electronic density on each amide proton gradually diminishes from the C-terminus to the N-terminus where two positive charges are present on the backbone and sidechain amine groups. The N-terminus is able to interact with negatively charged phosphate oxygen atoms in the interior of the bilayer, acting as an arrow. After an initial electrostatic attraction, the negatively charged residues E4 and D8 form salt bridges with the amine moieties of PE, whose flexibility and poor hindrance facilitate the folding of Sesquin in an amphipathic alpha helix. In the final step, the apolar side of the helix drops into the interior of the target bilayer and Sesquin remains anchored to the phosphate groups, while occupying the layer underneath. In the case of phosphatidylcholine membranes, the presence of methyl groups in the amine of choline might account for the impossibility to form salt bridges with E4 and D8 while their increased steric hindrance might prevent the insertion of the helix.

Our data clearly show a remarkable selectivity of Sesquin for ergosterol containing membranes, thus explaining its main antifungal activity and making it a good candidate for food preservation. Its activity does not seem to be hampered by the use of common preservation techniques, possibly allowing its use for a synergistic antimicrobial action.

Abbreviations

AMPs: antimicrobial peptides; DPC: Dodecylphosphocholine; ssNMR: solid-state NMR; NMP: N-methyl-2-pyrrolidone; HBTU: 2-(1H-benzotriazol-1-yl)-1,1,3,3-tetramethyluronium hexafluorophosphate; DIEA: N,N-diisopropylethylamine; TFA: trifluoroacetic acid; PE: phosphatidylethanolamine; PG: phosphatidylglycerol; PI: phosphatidylinositol; PS: phosphatidylserine; CL: cardiolipin; NPT: isothermal-isobaric ensemble ; LINCS: LINear Constraint Solver; PBC: Periodic Boundary Conditions; PME: particle mesh Ewald; RMSD: root-mean-square deviation; TSP-d4: Deuterated sodium 3-(trimethylsilyl)propionate-d4; DPC: dodecylphosphocholine; DMPC: 1,2-dimyristoyl-sn-glycero-3-phosphocholine; DHPC: 1,2-dihexanoyl-sn-glycero-3-phosphocholine; DMPG: 1,2-dimyristoyl-sn-glycero-3-phospho-(1'-rac-glycerol); DMPS: 1,2-dimyristoyl-sn-glycero-3-phospho-L-serine; DMPE: 1,2-dimyristoyl-sn-glycero-3-phosphoethanolamine; MLV: multilamellar vesicles; POPC: 1-palmitoyl-2-oleoyl-glycero-3-phosphocholine; POPG: 1-palmitoyl-2-oleoyl-sn-glycero-3-phospho-(1'-rac-glycerol); POPS: 1-palmitoyl-2-oleoyl-sn-glycero-3-phospho-L-serine; POPE: 1-palmitoyl-2-oleoyl-sn-glycero-3-phosphoethanolamine; POPI: 1-palmitoyl-2-oleoyl-sn-glycero-3-phosphoinositol; PI: L-α-phosphatidylinositol; IC_{50} :half maximal inhibitory concentration; ADAPTABLE: All-in-one Database of Antimicrobial Peptides clusTered in fAmilies for Boosted seLectivity and dEsign; SR: sequence-related family; CSI: Chemical Shift Index; DTT: dithiothreitol; TCEP: tris(2-carboxyethyl)phosphine; CHO: cholesterol; ERGO: ergosterol; SITO: sitosterol; STIGMA: stigmasterol; DOPC: 1,2-dioleoyl-sn-glycero-3-phosphocholine.

Acknowledgements

We would like to thank Habiba Hasnaoui for assistance in the sample preparation and NMR assignment. We also thank the Matrics platform at the University “Picardie Jules Verne” and the “Méso-centre de Calcul Scientifique Intensif” at the University of Lille for providing computing resources.

Funding

Francisco Ramos-Martíńs PhD scholarship was co-funded by Conseil régional des Hauts-de-France and by *European Fund for Economic and Regional Development* (FEDER); Claudia Herrera-León’s PhD scholarship was funded by the National Council for Science and Technology (CONACYT).

Competing interests

The authors declare that they have no competing interests.

CRediT authorship contribution statement

Francisco Ramos-Martín: Data curation, Formal analysis, Software, Investigation, Methodology, Writing - original draft, Writing - review & editing. Claudia Herrera-León: Investigation, Methodology, Writing - review & editing. Viviane Antonietti: Investigation. Pascal Sonnet: Writing - review & editing, Funding acquisition, Resources. Catherine Sarazin: Writing - review & editing, Funding acquisition, Resources. Nicola D'Amelio: Data curation, Formal analysis, Writing - review & editing, Validation, Software, Conceptualization, Funding acquisition, Supervision

Competing interests

The authors declare that they have no competing interests.

Appendix A. Supplementary data

The following are the Supplementary data to this article:

…

References

[1] J. Dijksterhuis, J. Houbraken, R.A. Samson, 2 Fungal Spoilage of Crops and Food, in: Agricultural Applications, Springer, Berlin, Heidelberg, 2013: pp. 35–56.

[2] J.I. Pitt, A.D. Hocking, Fresh and Perishable Foods, in: Fungi and Food Spoilage, Springer, Boston, MA, 2009: pp. 383–400.

[3] J.I. Pitt, A.D. Hocking, Spoilage of Stored, Processed and Preserved Foods, in: Fungi and Food Spoilage, Springer, Boston, MA, 2009: pp. 401–421.

[4] V. Heinz, R. Buckow, Food preservation by high pressure, Journal für Verbraucherschutz und Lebensmittelsicherheit. 5 (2009) 73–81.

[5] Y. Li, Z. Zheng, S. Zhu, H.S. Ramaswamy, Y. Yu, Effect of Low-Temperature-High-Pressure Treatment on the Reduction of in Milk, Foods. 9 (2020). https://doi.org/10.3390/foods9121742.

[6] B. Yang, Y. Shi, X. Xia, M. Xi, X. Wang, B. Ji, J. Meng, Inactivation of foodborne pathogens in raw milk using high hydrostatic pressure, Food Control. 28 (2012) 273–278.

[7] T. Domitrovic, C.M. Fernandes, E. Boy-Marcotte, E. Kurtenbach, High hydrostatic pressure activates gene expression through Msn2/4 stress transcription factors which are involved in the acquired tolerance by mild pressure precondition in Saccharomyces cerevisiae, FEBS Lett. 580 (2006) 6033–6038.

[8] T. Grahl, H. Märkl, Killing of microorganisms by pulsed electric fields, Appl. Microbiol. Biotechnol. 45 (1996) 148–157.

[9] L.D. Reina, Z.T. Jin, Q.H. Zhang, A.E. Yousef, Inactivation of Listeria monocytogenes in milk by pulsed electric field, J. Food Prot. 61 (1998). https://doi.org/10.4315/0362-028x-61.9.1203.

[10] H.W. Yeom, G.A. Evrendilek, Z.T. Jin, Q.H. Zhang, Processing of yogurt-based products with pulsed electric fields: Microbial, sensory and physical evaluations, J. Food Process. Preserv. 28 (2004) 161–178.

[11] Z.F. Bhat, J.D. Morton, S.L. Mason, A.E.-D.A. Bekhit, Current and future prospects for the use of pulsed electric field in the meat industry, Crit. Rev. Food Sci. Nutr. 59 (2019) 1660–1674.

[12] W. Chen, H. Hu, C. Zhang, F. Huang, D. Zhang, H. Zhang, Adaptation response of Pseudomonas fragi on refrigerated solid matrix to a moderate electric field, BMC Microbiol. 17 (2017) 32.

[13] P.K. Jha, E. Xanthakis, V. Jury, M. Havet, A. Le-Bail, Advances of electro-freezing in food processing, Current Opinion in Food Science. 23 (2018) 85–89. https://doi.org/10.1016/j.cofs.2018.06.007.

[14] T. Kang, Y. You, S. Jun, Supercooling preservation technology in food and biological samples: a review focused on electric and magnetic field applications, Food Sci. Biotechnol. 29 (2020) 303–321.

[15] Q. Wang, Y. Li, D.-W. Sun, Z. Zhu, Enhancing Food Processing by Pulsed and High Voltage Electric Fields:

Principles and Applications, Crit. Rev. Food Sci. Nutr. 58 (2018) 2285–2298.
[16] J.I. Pitt, A.D. Hocking, Fresh and Perishable Foods, in: Fungi and Food Spoilage, Springer, Boston, MA, 2009: pp. 383–400.
[17] M. Choquer, E. Fournier, C. Kunz, C. Levis, J.-M. Pradier, A. Simon, M. Viaud, Botrytis cinerea virulence factors: new insights into a necrotrophic and polyphageous pathogen, FEMS Microbiol. Lett. 277 (2007) 1–10.
[18] S.W. Hoogerwerf, E.P.W. Kets, J. Dijksterhuis, High-oxygen and high-carbon dioxide containing atmospheres inhibit growth of food associated moulds, Lett. Appl. Microbiol. 35 (2002) 419–422.
[19] R.G. Griffiths, J. Dancer, E. O'Neill, J.L. Harwood, Lipid composition of Botrytis cinerea and inhibition of its radiolabelling by the fungicide iprodione, New Phytol. 160 (2003) 199–207.
[20] C. Srinivas, D. Nirmala Devi, K. Narasimha Murthy, C.D. Mohan, T.R. Lakshmeesha, B. Singh, N.K. Kalagatur, S.R. Niranjana, A. Hashem, A.A. Alqarawi, B. Tabassum, E.F. Abd Allah, S. Chandra Nayaka, Fusarium oxysporum f. sp. lycopersici causal agent of vascular wilt disease of tomato: Biology to diversity-A review, Saudi J. Biol. Sci. 26 (2019) 1315–1324.
[21] A.L. Snowdon, Post-Harvest Diseases and Disorders of Fruits and Vegetables: Volume 1: General Introduction and Fruits, Taylor & Francis, 1990.
[22] A.E. Desjardins, Fusarium Mycotoxins: Chemistry, Genetics and Biology, Amer Phytopathological Society, 2006.
[23] J.I. Pitt, A.D. Hocking, Spoilage of Stored, Processed and Preserved Foods, in: Fungi and Food Spoilage, Springer, Boston, MA, 2009: pp. 401–421.
[24] J.H. Wong, T.B. Ng, Sesquin, a potent defensin-like antimicrobial peptide from ground beans with inhibitory activities toward tumor cells and HIV-1 reverse transcriptase, Peptides. 26 (2005) 1120–1126.
[25] D. Tago, H. Andersson, N. Treich, Pesticides and health: a review of evidence on health effects, valuation of risks, and benefit-cost analysis, Adv. Health Econ. Health Serv. Res. 24 (2014) 203–295.
[26] J. Wang, X. Dou, J. Song, Y. Lyu, X. Zhu, L. Xu, W. Li, A. Shan, Antimicrobial peptides: Promising alternatives in the post feeding antibiotic era, Med. Res. Rev. 39 (2019) 831–859.
[27] F.M. Nikoletta Hegedüs, Antifungal proteins: More than antimicrobials?, Fungal Biol. Rev. 26 (2013) 132.
[28] J.H. Wong, T.B. Ng, Gymnin, a potent defensin-like antifungal peptide from the Yunnan bean (Gymnocladus chinensis Baill), Peptides. 24 (2003) 963–968.
[29] P.H.K. Ngai, T.B. Ng, Coccinin, an antifungal peptide with antiproliferative and HIV-1 reverse transcriptase inhibitory activities from large scarlet runner beans, Peptides. 25 (2004) 2063–2068.
[30] S.L. Grage, M.-A. Sani, O. Cheneval, S.T. Henriques, C. Schalck, R. Heinzmann, J.S. Mylne, P.K. Mykhailiuk, S. Afonin, I.V. Komarov, F. Separovic, D.J. Craik, A.S. Ulrich, Orientation and Location of the Cyclotide Kalata B1 in Lipid Bilayers Revealed by Solid-State NMR, Biophys. J. 112 (2017) 630.
[31] M. Vestergaard, N.A. Berglund, P.-C. Hsu, C. Song, H. Koldsø, B. Schiøtt, M.S.P. Sansom, Structure and Dynamics of Cinnamycin-Lipid Complexes: Mechanisms of Selectivity for Phosphatidylethanolamine Lipids, ACS Omega. 4 (2019) 18889–18899.
[32] Sarah R Dennison, Manuela Mura, Frederick Harris, Leslie H G Morton, Andrei Zvelindovsky, David A Phoenix, The role of C-terminal amidation in the membrane interactions of the anionic antimicrobial peptide, maximin H5, Biochimica et Biophysica Acta (BBA) - Biomembranes. 1848 (2015) 1111–1118.
[33] D.A. Phoenix, F. Harris, M. Mura, S.R. Dennison, The increasing role of phosphatidylethanolamine as a lipid receptor in the action of host defence peptides, Prog. Lipid Res. 59 (2015) 26–37.
[34] M.C. Larson, M.S. Karafin, C.A. Hillery, N. Hogg, Phosphatidylethanolamine is progressively exposed on RBCs during storage, Transfus. Med. 27 (2017) 136.
[35] F. Ramos-Martín, T. Annaval, S. Buchoux, C. Sarazin, N. D'Amelio, ADAPTABLE: a comprehensive web platform of antimicrobial peptides tailored to the user's research, Life Sci Alliance. 2 (2019). https://doi.org/10.26508/lsa.201900512.
[36] S. Jo, J.B. Lim, J.B. Klauda, W. Im, CHARMM-GUI Membrane Builder for mixed bilayers and its application to yeast membranes, Biophys. J. 97 (2009) 50–58.
[37] J. Lee, X. Cheng, J.M. Swails, M.S. Yeom, P.K. Eastman, J.A. Lemkul, S. Wei, J. Buckner, J.C. Jeong, Y. Qi, S. Jo, V.S. Pande, D.A. Case, C.L. Brooks 3rd, A.D. MacKerell Jr, J.B. Klauda, W. Im, CHARMM-GUI Input Generator for NAMD, GROMACS, AMBER, OpenMM, and CHARMM/OpenMM Simulations Using the CHARMM36 Additive Force Field, J. Chem. Theory Comput. 12 (2016) 405–413.
[38] E.L. Wu, X. Cheng, S. Jo, H. Rui, K.C. Song, E.M. Dávila-Contreras, Y. Qi, J. Lee, V. Monje-Galvan, R.M. Venable, J.B. Klauda, W. Im, CHARMM-GUI Membrane Builder toward realistic biological membrane simulations, J. Comput. Chem. 35 (2014) 1997–2004.
[39] S. Singh, K. Chaudhary, S.K. Dhanda, S. Bhalla, S.S. Usmani, A. Gautam, A. Tuknait, P. Agrawal, D. Mathur,

G.P.S. Raghava, SATPdb: a database of structurally annotated therapeutic peptides, Nucleic Acids Res. 44 (2016) D1119–26.
[40] M.J. Abraham, T. Murtola, R. Schulz, S. Páll, J.C. Smith, B. Hess, E. Lindahl, GROMACS: High performance molecular simulations through multi-level parallelism from laptops to supercomputers, SoftwareX. 1-2 (2015) 19–25. https://doi.org/10.1016/j.softx.2015.06.001.
[41] J.B. Klauda, R.M. Venable, J.A. Freites, J.W. O'Connor, D.J. Tobias, C. Mondragon-Ramirez, I. Vorobyov, A.D. MacKerell Jr, R.W. Pastor, Update of the CHARMM all-atom additive force field for lipids: validation on six lipid types, J. Phys. Chem. B. 114 (2010) 7830–7843.
[42] J. Huang, S. Rauscher, G. Nawrocki, T. Ran, M. Feig, B.L. de Groot, H. Grubmüller, A.D. MacKerell, CHARMM36m: an improved force field for folded and intrinsically disordered proteins, Nat. Methods. 14 (2016) 71–73.
[43] S. Jo, T. Kim, W. Im, Automated builder and database of protein/membrane complexes for molecular dynamics simulations, PLoS One. 2 (2007) e880.
[44] X. Cheng, S. Jo, H.S. Lee, J.B. Klauda, W. Im, CHARMM-GUI micelle builder for pure/mixed micelle and protein/micelle complex systems, J. Chem. Inf. Model. 53 (2013) 2171–2180.
[45] H.J.C. Berendsen, J.P.M. Postma, W.F. van Gunsteren, J. Hermans, Interaction Models for Water in Relation to Protein Hydration, The Jerusalem Symposia on Quantum Chemistry and Biochemistry. (1981) 331–342. https://doi.org/10.1007/978-94-015-7658-1_21.
[46] H.J.C. Berendsen, J.P.M. Postma, W.F. van Gunsteren, A. DiNola, J.R. Haak, Molecular dynamics with coupling to an external bath, The Journal of Chemical Physics. 81 (1984) 3684–3690. https://doi.org/10.1063/1.448118.
[47] M. Parrinello, A. Rahman, Polymorphic transitions in single crystals: A new molecular dynamics method, Journal of Applied Physics. 52 (1981) 7182–7190. https://doi.org/10.1063/1.328693.
[48] S. Nosé, M.L. Klein, Constant pressure molecular dynamics for molecular systems, Molecular Physics. 50 (1983) 1055–1076. https://doi.org/10.1080/00268978300102851.
[49] S. Nosé, A unified formulation of the constant temperature molecular dynamics methods, The Journal of Chemical Physics. 81 (1984) 511–519. https://doi.org/10.1063/1.447334.
[50] W.G. Hoover, Canonical dynamics: Equilibrium phase-space distributions, Phys. Rev. A Gen. Phys. 31 (1985) 1695–1697.
[51] W. Ding, M. Palaiokostas, G. Shahane, W. Wang, M. Orsi, Effects of High Pressure on Phospholipid Bilayers, J. Phys. Chem. B. 121 (2017) 9597–9606.
[52] Lindahl, Abraham, Hess, V. der Spoel, GROMACS 2019 Manual, (2018). https://doi.org/10.5281/zenodo.2424486.
[53] U. Essmann, L. Perera, M.L. Berkowitz, T. Darden, H. Lee, L.G. Pedersen, A smooth particle mesh Ewald method, The Journal of Chemical Physics. 103 (1995) 8577–8593. https://doi.org/10.1063/1.470117.
[54] D.J. Smith, J.B. Klauda, A.J. Sodt, Simulation Best Practices for Lipid Membranes [Article v1.0], Living Journal of Computational Molecular Science. 1 (2019). https://doi.org/10.33011/livecoms.1.1.5966.
[55] J. Lemkul, From Proteins to Perturbed Hamiltonians: A Suite of Tutorials for the GROMACS-2018 Molecular Simulation Package [Article v1.0], Living Journal of Computational Molecular Science. 1 (2019). https://doi.org/10.33011/livecoms.1.1.5068.
[56] S. Buchoux, FATSLiM: a fast and robust software to analyze MD simulations of membranes, Bioinformatics. 33 (2017) 133–134.
[57] R. Koradi, M. Billeter, K. Wüthrich, MOLMOL: a program for display and analysis of macromolecular structures, J. Mol. Graph. 14 (1996) 51–5, 29–32.
[58] W. Humphrey, A. Dalke, K. Schulten, VMD: Visual molecular dynamics, Journal of Molecular Graphics. 14 (1996) 33–38. https://doi.org/10.1016/0263-7855(96)00018-5.
[59] P.K. Janert, Gnuplot in Action: Understanding Data with Graphs, Manning Publications, 2010.
[60] W.L. DeLano, Pymol: An open-source molecular graphics tool, CCP4 Newsletter on Protein Crystallography. 40 (2002) 82–92.
[61] J.T. Nielsen, F.A.A. Mulder, POTENCI: prediction of temperature, neighbor and pH-corrected chemical shifts for intrinsically disordered proteins, J. Biomol. NMR. 70 (2018) 141–165.
[62] I. Marcotte, M. Auger, Bicelles as model membranes for solid-and solution-state NMR studies of membrane peptides and proteins, Concepts in Magnetic Resonance Part A: An Educational Journal. 24 (2005) 17–37.
[63] H. Ghimire, J.J. Inbaraj, G.A. Lorigan, A comparative study of the effect of cholesterol on bicelle model membranes using X-band and Q-band EPR spectroscopy, Chem. Phys. Lipids. 160 (2009) 98–104.
[64] H. Sasaki, S. Fukuzawa, J. Kikuchi, S. Yokoyama, H. Hirota, K. Tachibana, Cholesterol Doping Induced

Enhanced Stability of Bicelles, Langmuir. 19 (2003) 9841–9844.
[65] A. Diller, C. Loudet, F. Aussenac, G. Raffard, S. Fournier, M. Laguerre, A. Grélard, S.J. Opella, F.M. Marassi, E.J. Dufourc, Bicelles: A natural "molecular goniometer" for structural, dynamical and topological studies of molecules in membranes, Biochimie. 91 (2009) 744–751.
[66] N. Monnier, A.L. Furlan, S. Buchoux, M. Deleu, M. Dauchez, S. Rippa, C. Sarazin, Exploring the Dual Interaction of Natural Rhamnolipids with Plant and Fungal Biomimetic Plasma Membranes through Biophysical Studies, Int. J. Mol. Sci. 20 (2019). https://doi.org/10.3390/ijms20051009.
[67] A.L. Furlan, A. Castets, F. Nallet, I. Pianet, A. Grélard, E.J. Dufourc, J. Géan, Red wine tannins fluidify and precipitate lipid liposomes and bicelles. A role for lipids in wine tasting?, Langmuir. 30 (2014) 5518–5526.
[68] A.L. Furlan, M.-L. Jobin, I. Pianet, E.J. Dufourc, J. Géan, Flavanol/lipid interaction: a novel molecular perspective in the description of wine astringency & bitterness and antioxidant action, Tetrahedron. 71 (2015) 3143–3147. https://doi.org/10.1016/j.tet.2014.07.106.
[69] A. Grélard, P. Guichard, P. Bonnafous, S. Marco, O. Lambert, C. Manin, F. Ronzon, E.J. Dufourc, Hepatitis B subvirus particles display both a fluid bilayer membrane and a strong resistance to freeze drying: a study by solid-state NMR, light scattering, and cryo-electron microscopy/tomography, The FASEB Journal. 27 (2013) 4316–4326. https://doi.org/10.1096/fj.13-232843.
[70] L. 'celia Hall, E. Donovan, M. Araya, E. Idowa, I. Jiminez-Segovia, A. Folck, C.D. Wells, A.C. Kimble-Hill, Identification of Specific Lysines and Arginines That Mediate Angiomotin Membrane Association, ACS Omega. 4 (2019) 6726–6736.
[71] J.H. Davis, K.R. Jeffrey, M. Bloom, M.I. Valic, T.P. Higgs, Quadrupolar echo deuteron magnetic resonance spectroscopy in ordered hydrocarbon chains, Chemical Physics Letters. 42 (1976) 390–394. https://doi.org/10.1016/0009-2614(76)80392-2.
[72] S. Soltani, K. Keymanesh, S. Sardari, In silico analysis of antifungal peptides, Expert Opin. Drug Discov. 2 (2007). https://doi.org/10.1517/17460441.2.6.837.
[73] D.S. Wishart, B.D. Sykes, F.M. Richards, The chemical shift index: a fast and simple method for the assignment of protein secondary structure through NMR spectroscopy, Biochemistry. 31 (1992) 1647–1651.
[74] D.S. Wishart, B.D. Sykes, The 13 C Chemical-Shift Index: A simple method for the identification of protein secondary structure using 13 C chemical-shift data, J. Biomol. NMR. 4 (1994) 171–180.
[75] D.S. Wishart, Interpreting protein chemical shift data, Prog. Nucl. Magn. Reson. Spectrosc. 58 (2011) 62–87.
[76] Y. Wang, O. Jardetzky, Probability-based protein secondary structure identification using combined NMR chemical-shift data, Protein Sci. 11 (2002) 852–861.
[77] A.R. Mól, M.S. Castro, W. Fontes, NetWheels: A web application to create high quality peptide helical wheel and net projections, Cold Spring Harbor Laboratory. (2018) 416347. https://doi.org/10.1101/416347.
[78] D. Sharma, K. Rajarathnam, 13C NMR chemical shifts can predict disulfide bond formation, J. Biomol. NMR. 18 (2000) 165–171.
[79] D. Liu, J. Liu, J. Li, L. Xia, J. Yang, S. Sun, J. Ma, F. Zhang, A potential food biopreservative, CecXJ-37N, non-covalently intercalates into the nucleotides of bacterial genomic DNA beyond membrane attack, Food Chem. 217 (2017) 576–584.
[80] F. Ramos-Martín, C. Herrera-León, V. Antonietti, P. Sonnet, C. Sarazin, N. D'Amelio, Antimicrobial Peptide K11 Selectively Recognizes Bacterial Biomimetic Membranes and Acts by Twisting Their Bilayers, Pharmaceuticals . 14 (2020) 1.
[81] F. Porcelli, A. Ramamoorthy, G. Barany, G. Veglia, On the role of NMR spectroscopy for characterization of antimicrobial peptides, Methods Mol. Biol. 1063 (2013) 159–180.
[82] J.H. Davis, The description of membrane lipid conformation, order and dynamics by 2H-NMR, Biochim. Biophys. Acta. 737 (1983) 117–171.
[83] T.R. Molugu, S. Lee, M.F. Brown, Concepts and Methods of Solid-State NMR Spectroscopy Applied to Biomembranes, Chem. Rev. 117 (2017) 12087–12132.
[84] E.S. Salnikov, A.J. Mason, B. Bechinger, Membrane order perturbation in the presence of antimicrobial peptides by (2)H solid-state NMR spectroscopy, Biochimie. 91 (2009) 734–743.
[85] N. Harmouche, B. Bechinger, Lipid-Mediated Interactions between the Antimicrobial Peptides Magainin 2 and PGLa in Bilayers, Biophys. J. 115 (2018) 1033–1044.
[86] K. Matsuzaki, O. Murase, H. Tokuda, S. Funakoshi, N. Fujii, K. Miyajima, Orientational and aggregational states of magainin 2 in phospholipid bilayers, Biochemistry. 33 (1994) 3342–3349.
[87] C. Aisenbrey, A. Marquette, B. Bechinger, The Mechanisms of Action of Cationic Antimicrobial Peptides

Refined by Novel Concepts from Biophysical Investigations, Adv. Exp. Med. Biol. 1117 (2019) 33–64.
[88] E.J. Dufourc, J. Dufourcq, T.H. Birkbeck, J.H. Freer, Delta-haemolysin from Staphylococcus aureus and model membranes. A solid-state 2H-NMR and 31P-NMR study, Eur. J. Biochem. 187 (1990). https://doi.org/10.1111/j.1432-1033.1990.tb15340.x.
[89] E.J. Dufourc, I.C. Smith, J. Dufourcq, Molecular details of melittin-induced lysis of phospholipid membranes as revealed by deuterium and phosphorus NMR, Biochemistry. 25 (1986) 6448–6455.
[90] F. Jean-François, S. Castano, B. Desbat, B. Odaert, M. Roux, M.-H. Metz-Boutigue, E.J. Dufourc, Aggregation of cateslytin beta-sheets on negatively charged lipids promotes rigid membrane domains. A new mode of action for antimicrobial peptides?, Biochemistry. 47 (2008) 6394–6402.
[91] W. Zhang, S.O. Smith, Mechanism of penetration of Antp(43-58) into membrane bilayers, Biochemistry. 44 (2005) 10110–10118.
[92] A.M. Sendecki, M.F. Poyton, A.J. Baxter, T. Yang, P.S. Cremer, Supported Lipid Bilayers with Phosphatidylethanolamine as the Major Component, Langmuir. 33 (2017) 13423–13429.
[93] R.N.A.H. Lewis, R.N. McElhaney, The physicochemical properties of cardiolipin bilayers and cardiolipin-containing lipid membranes, Biochim. Biophys. Acta. 1788 (2009) 2069–2079.
[94] A. Tari, L. Huang, Structure and function relationship of phosphatidylglycerol in the stabilization of phosphatidylethanolamine bilayer, Biochemistry. 28 (1989) 7708–7712. https://doi.org/10.1021/bi00445a028.
[95] F. Szoka Jr, D. Papahadjopoulos, Comparative properties and methods of preparation of lipid vesicles (liposomes), Annu. Rev. Biophys. Bioeng. 9 (1980) 467–508.
[96] D. Papahadjopoulos, N. Miller, Phospholipid model membranes. I. Structural characteristics of hydrated liquid crystals, Biochim. Biophys. Acta. 135 (1967) 624–638.
[97] B.J. Litman, Lipid model membranes. Characterization of mixed phospholipid vesicles, Biochemistry. 12 (1973) 2545–2554.
[98] D.O. Tinker, L. Pinteric, On the identification of lamellar and hexagonal phases in negatively stained phospholipid-water systems, Biochemistry. 10 (1971) 860–865.
[99] E. Junger, H. Reinauer, Liquid crystalline phases of hydrated phosphatidylethanolamine, Biochim. Biophys. Acta. 183 (1969) 304–308.
[100] P. Perczyk, A. Wójcik, P. Wydro, M. Broniatowski, The role of phospholipid composition and ergosterol presence in the adaptation of fungal membranes to harsh environmental conditions-membrane modeling study, Biochim. Biophys. Acta Biomembr. 1862 (2020) 183136.
[101] K. Thevissen, K.K.A. Ferket, I.E.J.A. François, B.P.A. Cammue, Interactions of antifungal plant defensins with fungal membrane components, Peptides. 24 (2003) 1705–1712.
[102] D.M. Lösel, Lipids in the Structure and Function of Fungal Membranes, in: Biochemistry of Cell Walls and Membranes in Fungi, Springer, Berlin, Heidelberg, 1990: pp. 119–133.
[103] A. Makovitzki, D. Avrahami, Y. Shai, Ultrashort antibacterial and antifungal lipopeptides, Proc. Natl. Acad. Sci. U. S. A. 103 (2006) 15997–16002.
[104] J.D. Weete, Lipid Biochemistry of Fungi and Other Organisms, Springer Science & Business Media, 2012.
[105] S. Shrestha, M. Grilley, M.Y. Fosso, C.-W.T. Chang, J.Y. Takemoto, Membrane lipid-modulated mechanism of action and non-cytotoxicity of novel fungicide aminoglycoside FG08, PLoS One. 8 (2013) e73843.
[106] D. Avrahami, Y. Shai, A new group of antifungal and antibacterial lipopeptides derived from non-membrane active peptides conjugated to palmitic acid, J. Biol. Chem. 279 (2004) 12277–12285.
[107] H. Watson, Biological membranes, Essays Biochem. 59 (2015) 43–69.
[108] C. Galanth, F. Abbassi, O. Lequin, J. Ayala-Sanmartin, A. Ladram, P. Nicolas, M. Amiche, Mechanism of antibacterial action of dermaseptin B2: interplay between helix-hinge-helix structure and membrane curvature strain, Biochemistry. 48 (2009) 313–327.
[109] T. Romantsov, Z. Guan, J.M. Wood, Cardiolipin and the osmotic stress responses of bacteria, Biochim. Biophys. Acta. 1788 (2009) 2092–2100.
[110] S.C. Lopes, C.S. Neves, P. Eaton, P. Gameiro, Improved model systems for bacterial membranes from differing species: the importance of varying composition in PE/PG/cardiolipin ternary mixtures, Mol. Membr. Biol. 29 (2012) 207–217.
[111] K. Murzyn, T. Róg, M. Pasenkiewicz-Gierula, Phosphatidylethanolamine-phosphatidylglycerol bilayer as a model of the inner bacterial membrane, Biophys. J. 88 (2005) 1091–1103.
[112] R.N.A.H. Lewis, R.N. McElhaney, The physicochemical properties of cardiolipin bilayers and cardiolipin-containing lipid membranes, Biochim. Biophys. Acta. 1788 (2009) 2069–2079.

[113] Z. Yang, H. Choi, J.C. Weisshaar, Melittin-Induced Permeabilization, Re-sealing, and Re-permeabilization of E. coli Membranes, Biophys. J. 114 (2018) 368–379.
[114] F.G. Avci, B.S. Akbulut, E. Ozkirimli, Membrane Active Peptides and Their Biophysical Characterization, Biomolecules. 8 (2018). https://doi.org/10.3390/biom8030077.
[115] M. Orsi, M.G. Noro, J.W. Essex, Dual-resolution molecular dynamics simulation of antimicrobials in biomembranes, J. R. Soc. Interface. 8 (2011) 826–841.
[116] J. Kästner, Umbrella sampling: Umbrella sampling, Wiley Interdiscip. Rev. Comput. Mol. Sci. 1 (2011) 932–942.
[117] A. Barducci, M. Bonomi, M. Parrinello, Metadynamics: Metadynamics, Wiley Interdiscip. Rev. Comput. Mol. Sci. 1 (2011) 826–843.
[118] S.J. Marrink, V. Corradi, P.C.T. Souza, H.I. Ingólfsson, D.P. Tieleman, M.S.P. Sansom, Computational Modeling of Realistic Cell Membranes, Chem. Rev. 119 (2019) 6184–6226.
[119] T. Mori, N. Miyashita, W. Im, M. Feig, Y. Sugita, Molecular dynamics simulations of biological membranes and membrane proteins using enhanced conformational sampling algorithms, Biochim. Biophys. Acta. 1858 (2016) 1635–1651.
[120] M. Lorizate, T. Sachsenheimer, B. Glass, A. Habermann, M.J. Gerl, H.-G. Kräusslich, B. Brügger, Comparative lipidomics analysis of HIV-1 particles and their producer cell membrane in different cell lines, Cell. Microbiol. 15 (2013) 292–304.
[121] B. Brügger, B. Glass, P. Haberkant, I. Leibrecht, F.T. Wieland, H.-G. Kräusslich, The HIV lipidome: a raft with an unusual composition, Proc. Natl. Acad. Sci. U. S. A. 103 (2006) 2641–2646.
[122] S.T. Henriques, Y.-H. Huang, M.A.R.B. Castanho, L.A. Bagatolli, S. Sonza, G. Tachedjian, N.L. Daly, D.J. Craik, Phosphatidylethanolamine binding is a conserved feature of cyclotide-membrane interactions, J. Biol. Chem. 287 (2012) 33629–33643.
[123] S.T. Henriques, Y.-H. Huang, K. Johan Rosengren, H.G. Franquelim, F.A. Carvalho, A. Johnson, S. Sonza, G. Tachedjian, Miguel A R, N.L. Daly, D.J. Craik, Decoding the Membrane Activity of the Cyclotide Kalata B1, Journal of Biological Chemistry. 286 (2011) 24231–24241. https://doi.org/10.1074/jbc.m111.253393.
[124] J.H. Stafford, P.E. Thorpe, Increased exposure of phosphatidylethanolamine on the surface of tumor vascular endothelium, Neoplasia. 13 (2011) 299–308.
[125] R.J.P. Musters, R.J. Ph. Musters, E. Pröbstl-Biegelmann, T.A.B. Van Veen, K.H.N. Hoebe, J.A.F.O. Den Kamp, A.J. Verkleij, J.A. Post, Sarcolemmal phosphatidylethanolamine reorganization during simulated ischaemia and reperfusion, Molecular Membrane Biology. 13 (1996) 159–164. https://doi.org/10.3109/09687689609160592.
[126] X. Zhou, J. Mao, J. Ai, Y. Deng, M.R. Roth, C. Pound, J. Henegar, R. Welti, S.A. Bigler, Identification of plasma lipid biomarkers for prostate cancer by lipidomics and bioinformatics, PLoS One. 7 (2012) e48889.
[127] K. Emoto, N. Toyama-Sorimachi, H. Karasuyama, K. Inoue, M. Umeda, Exposure of phosphatidylethanolamine on the surface of apoptotic cells, Exp. Cell Res. 232 (1997) 430–434.
[128] J.N. Valitova, A.G. Sulkarnayeva, F.V. Minibayeva, Plant Sterols: Diversity, Biosynthesis, and Physiological Functions, Biochemistry . 81 (2016) 819–834.
[129] S.L. Grage, S. Afonin, S. Kara, G. Buth, A.S. Ulrich, Membrane Thinning and Thickening Induced by Membrane-Active Amphipathic Peptides, Front Cell Dev Biol. 4 (2016) 65.
[130] K.L. Horton, K.M. Stewart, S.B. Fonseca, Q. Guo, S.O. Kelley, Mitochondria-penetrating peptides, Chem. Biol. 15 (2008). https://doi.org/10.1016/j.chembiol.2008.03.015.
[131] J.-P. Douliez, L. Navailles, E.J. Dufourc, F. Nallet, Fully deuterated magnetically oriented system based on fatty acid direct hexagonal phases, Langmuir. 30 (2014) 5075–5081.
[132] R.E. Brown, Sphingolipid organization in biomembranes: what physical studies of model membranes reveal, J. Cell Sci. 111 (Pt 1) (1998) 1–9.
[133] G. Chen, K. Huang, M. Miao, B. Feng, O.H. Campanella, Molecular Dynamics Simulation for Mechanism Elucidation of Food Processing and Safety: State of the Art, Compr. Rev. Food Sci. Food Saf. 18 (2019) 243–263.
[134] S. Sun, J.T.Y. Wong, T.-Y. Zhang, Molecular dynamics simulations of phase transition of lamellar lipid membrane in water under an electric field, Soft Matter. 7 (2010) 147–152.
[135] B. Wang, J. Zhang, Y. Zhang, Z. Mao, N. Lu, Q.H. Liu, The penetration of a charged peptide across a membrane under an external electric field: a coarse-grained molecular dynamics simulation, RSC Adv. 8 (2018) 41517–41525.
[136] N. Machado, C. Callegaro, M.A. Christoffolete, H. Martinho, Tuning the transdermal transport by application of external continuous electric field: a coarse-grained molecular dynamics study, Phys. Chem. Chem. Phys. (2021). https://doi.org/10.1039/D1CP00354B.

[137] Z. Kong, H. Wang, L. Liang, Z. Zhang, S. Ying, Q. Hu, J.W. Shen, Investigation of the morphological transition of a phospholipid bilayer membrane in an external electric field via molecular dynamics simulation, J. Mol. Model. 23 (2017). https://doi.org/10.1007/s00894-017-3292-1.
[138] J.R. Silvius, Thermotropic phase transitions of pure lipids in model membranes and their modifications by membrane proteins, Lipid-Protein Interactions. 2 (1982) 239–281.
[139] M. Kranenburg, B. Smit, Phase behavior of model lipid bilayers, J. Phys. Chem. B. 109 (2005) 6553–6563.
[140] M. Ritz, J.L. Tholozan, M. Federighi, M.F. Pilet, Physiological damages of Listeria monocytogenes treated by high hydrostatic pressure, Int. J. Food Microbiol. 79 (2002). https://doi.org/10.1016/s0168-1605(02)00178-2.
[141] V. Heinz, R. Buckow, Food preservation by high pressure, Journal für Verbraucherschutz und Lebensmittelsicherheit. 5 (2009) 73–81.
[142] J. Dijksterhuis, R.A. Samson, Activation of ascospores by novel food preservation techniques, Adv. Exp. Med. Biol. 571 (2006) 247–260.
[143] D. Knorr, V. Heinz, R. Buckow, High pressure application for food biopolymers, Biochim. Biophys. Acta. 1764 (2006). https://doi.org/10.1016/j.bbapap.2006.01.017.
[144] T. Norton, D.-W. Sun, Recent Advances in the Use of High Pressure as an Effective Processing Technique in the Food Industry, Food Bioprocess Technol. 1 (2007) 2–34.
[145] Fungi in Extreme Environments, in: The Mycota, Springer Berlin Heidelberg, Berlin, Heidelberg, 2007: pp. 85–103.
[146] L.P. Gaspar, A.C. Silva, A.M. Gomes, M.S. Freitas, A.B. Ap, W.D. Schwarcz, J. Mestecky, M.J. Novak, D. Foguel, J.L. Silva, Hydrostatic pressure induces the fusion-active state of enveloped viruses, J. Biol. Chem. 277 (2002). https://doi.org/10.1074/jbc.M106096200.
[147] M. Sharma, K.E. Kniel, A. Derevianko, J. Ling, A.A. Bhagwat, Sensitivity of Escherichia albertii, a Potential Food-Borne Pathogen, to Food Preservation Treatments, Appl. Environ. Microbiol. 73 (2007) 4351.
[148] K.A. Karatzas, M.H. Bennik, Characterization of a Listeria monocytogenes Scott A isolate with high tolerance towards high hydrostatic pressure, Appl. Environ. Microbiol. 68 (2002). https://doi.org/10.1128/aem.68.7.3183-3189.2002.
[149] T. Domitrovic, C.M. Fernandes, E. Boy-Marcotte, E. Kurtenbach, High hydrostatic pressure activates gene expression through Msn2/4 stress transcription factors which are involved in the acquired tolerance by mild pressure precondition in Saccharomyces cerevisiae, FEBS Lett. 580 (2006) 6033–6038.
[150] M.C. Teixeira, N.P. Mira, I. Sá-Correia, A genome-wide perspective on the response and tolerance to food-relevant stresses in Saccharomyces cerevisiae, Curr. Opin. Biotechnol. 22 (2011). https://doi.org/10.1016/j.copbio.2010.10.011.
[151] Z.F. Bhat, J.D. Morton, S.L. Mason, A.E.-D.A. Bekhit, Current and future prospects for the use of pulsed electric field in the meat industry, Crit. Rev. Food Sci. Nutr. 59 (2019) 1660–1674.
[152] M. Pal, Pulsed electric field processing: An emerging technology for food preservation, J. Exp. Food Chem. 03 (2017). https://doi.org/10.4172/2472-0542.1000126.
[153] T. Grahl, H. Märkl, Killing of microorganisms by pulsed electric fields, Appl. Microbiol. Biotechnol. 45 (1996) 148–157.
[154] L.D. Reina, Z.T. Jin, Q.H. Zhang, A.E. Yousef, Inactivation of Listeria monocytogenes in milk by pulsed electric field, J. Food Prot. 61 (1998). https://doi.org/10.4315/0362-028x-61.9.1203.
[155] W. Chen, H. Hu, C. Zhang, F. Huang, D. Zhang, H. Zhang, Adaptation response of Pseudomonas fragi on refrigerated solid matrix to a moderate electric field, BMC Microbiol. 17 (2017) 32.
[156] T. Kang, Y. You, S. Jun, Supercooling preservation technology in food and biological samples: a review focused on electric and magnetic field applications, Food Sci. Biotechnol. 29 (2020) 303–321.